

Characterizing Gaussian quantum processes with Gaussian resources*

Logan W. Grove¹, Pratik J. Barge², and Kevin Valson Jacob¹

¹ *Department of Physics and Engineering, Wheaton College, Wheaton, IL 60187 and*

² *Department of Physics, Washington University in St Louis, MO, 63105*

(Dated: March 21, 2025)

Characterizing quantum processes is indispensable for the implementation of any task in quantum information processing. In this paper, we develop an efficient method to fully characterize arbitrary Gaussian processes in continuous-variable quantum systems. This is done by directly obtaining all elements of the symplectic matrix that describes the process. Only Gaussian resources such as coherent probes and quadrature measurements are needed for this task. The method is efficient, involving only $O(N^2)$ steps to characterize an N -mode system. Further, the method is resilient to uniform loss. We simulate this procedure using the Python package Strawberry Fields. We observe that heterodyne measurements outperform homodyne measurements for reconstructing Gaussian processes.

I. INTRODUCTION

A variety of tasks in quantum information science can be implemented by continuous variable systems, of which quantum light is a leading platform [1, 2]. Such implementations necessitate the production, transformation, and detection of quantum light. Recently, several platforms have been developed for these tasks [3, 4]. Due to manufacturing imperfections, a post-production characterization of these technologies is necessary to ensure that such devices function as intended [5].

Characterizing continuous variable systems can be inherently challenging, as the Hilbert space corresponding to such systems is infinite-dimensional [6]. However, a simplification is possible when we restrict our attention to Gaussian systems. These systems include linear optical systems as well as those with quadratic nonlinearities such as parametric amplifiers and down-converters, and squeezers [7, 8]. Despite this restriction, Gaussian systems enable the execution of several important quantum information tasks including communication, cryptography, teleportation, and non-universal quantum computation such as Gaussian boson sampling [6].

Gaussian evolutions are generated by Hamiltonians that are at most quadratic in the mode operators. These evolutions map Gaussian states —described by their first and second moments alone—to Gaussian states. Therefore, characterizing an N -mode Gaussian evolution necessitates the finding of $O(N^2)$ parameters.

A general scheme to characterize quantum devices consists of three steps. First, well-characterized quantum states are prepared. Subsequently, these states are used to probe the uncharacterized device. Finally, a specified set of measurements is performed on the states after they have evolved through the device. From the outcomes of these measurements, one then deduces the complete description of the unknown device.

Several investigations have focused on characterizing

linear optical systems by determining their $N \times N$ unitary transfer matrix. This was done using non-Gaussian probes in Refs. [9–12], and with Gaussian probes in Refs. [13–15]. However, these schemes assumed that the unitary matrix is real-bordered, i.e. the elements in its first row and first column are real. This restriction was removed in Ref. [16], which considered not only linear optical systems but also those with quadratic non-linearities i.e. all Gaussian systems. However, non-classical probes were still used in this analysis.

Several other works have explored beyond linear optics by characterizing all Gaussian systems. In Ref. [17], the Husimi Q-function corresponding to the Gaussian process was found using coherent probes. In contrast, coherent probes and photon number-resolving measurements were used to directly find the parameters of the Gaussian map in Ref. [18]. Ref. [19] uses coherent states and heterodyne measurements to characterize a single-mode Gaussian process.

Despite this progress, a method that directly characterizes multi-mode Gaussian processes with only Gaussian resources such as coherent probes and quadrature detection is still needed. In this paper, we develop such a method. Using this method, we directly obtain all elements of the symplectic matrix that completely describes the process.

This paper is structured as follows: In section II, we outline the mathematical conventions used in this work. Then in section III, we give details of our proposed setup. Section IV then shows the procedure employed in our method. In section V, we incorporate loss in devices and demonstrate that the scheme is resilient to uniform loss. The results of simulating our method are presented in section VI. We discuss the results in section VII, and conclude in section VIII.

II. QUANTUM CONTINUOUS VARIABLE SYSTEMS

Consider a N -mode bosonic quantum system that has the corresponding mode annihilation and creation oper-

* kevin.valsonjacob@wheaton.edu

ators $\{\hat{a}_i, \hat{a}_i^\dagger\}_{i=1}^N$. These operators satisfy the commutation relation $[\hat{a}_i, \hat{a}_j^\dagger] = \delta_{ij}$. These operators can be used to define a set of quadrature operators for each mode as

$$\hat{X}_i = \frac{1}{\sqrt{2}} (\hat{a}_i + \hat{a}_i^\dagger), \quad \hat{P}_i = \frac{1}{\sqrt{2}i} (\hat{a}_i - \hat{a}_i^\dagger), \quad (1)$$

where the \hat{X} quadratures are called position operators, and the \hat{P} quadratures are called the momentum operators. These quadrature operators are Hermitian and as such have real eigenvalues which can be experimentally measured.

As there are $2N$ of these quadrature operators, we formally arrange these quadrature operators as a vector of $2N$ elements as

$$\hat{\mathbf{r}} \equiv (\hat{X}_1, \dots, \hat{X}_N, \hat{P}_1, \dots, \hat{P}_N)^T. \quad (2)$$

A. Gaussian States

A Gaussian state $\hat{\rho}$ of a continuous variable system is fully characterized by the first and second moments of the vector of quadrature operators. The first moment is called the mean vector and is defined as

$$\mathbf{r} \equiv \langle \hat{\mathbf{r}} \rangle = \text{Tr}(\hat{\mathbf{r}} \hat{\rho}). \quad (3)$$

The second moment, called the covariance matrix, is defined as

$$\sigma = \text{Tr}[\{(\hat{\mathbf{r}} - \mathbf{r}), (\hat{\mathbf{r}} - \mathbf{r})^T\} \hat{\rho}], \quad (4)$$

where $\{.,.\}$ represents the anti-commutator. Examples of Gaussian states are the vacuum state, coherent states, thermal states, and squeezed states [20].

B. Gaussian Processes

Gaussian quantum processes map Gaussian states to Gaussian states. Such processes include both passive transformations of the mode operators, as in the case of linear optics, and active transformations that do not preserve energy. We consider Gaussian processes that map the mean vector of a Gaussian state as

$$\mathbf{r}^{\text{out}} = S \mathbf{r}^{\text{in}}, \quad (5)$$

where S is a $2N \times 2N$ invertible symplectic matrix of real elements with determinant +1 [6, 21, 22]. Since S is symplectic, we have

$$SJS^T = J, \quad J = \begin{pmatrix} 0_N & \mathbb{1}_N \\ -\mathbb{1}_N & 0_N \end{pmatrix}. \quad (6)$$

Passive transformations

If the Gaussian quantum process corresponds to passive transformations of the mode operators, as in linear optics, the $2N \times 2N$ symplectic matrix S is related to a $N \times N$ unitary matrix U that transforms the mode operators of the linear optical system [23]. It is shown in Appendix A that U is related to S as

$$S_{\text{passive}} = \begin{pmatrix} \text{Re}(U) & \text{Im}(U) \\ -\text{Im}(U) & \text{Re}(U) \end{pmatrix}. \quad (7)$$

C. Gaussian measurements

A quantum measurement is defined to be a gaussian measurement if its application to a gaussian state yields a gaussian-distributed outcome [6]. Two common gaussian measurements are the homodyne and the heterodyne. Both of these are single-mode measurements that can be used to reconstruct the first moment (i.e. the mean vector) of a quantum state.

Homodyne detection is modeled as a projection onto the quadrature basis [6]. As such, it can measure any given quadrature of a quantum state at a time. In contrast, heterodyne detection is modeled as a projection onto the coherent basis. Thus, it jointly measures complementary quadratures and is subject to the unavoidable Heisenberg-Robertson-Schrödinger uncertainty [24].

III. SETUP

A schematic of the setup proposed to characterize the Gaussian process is shown in Fig. 1.

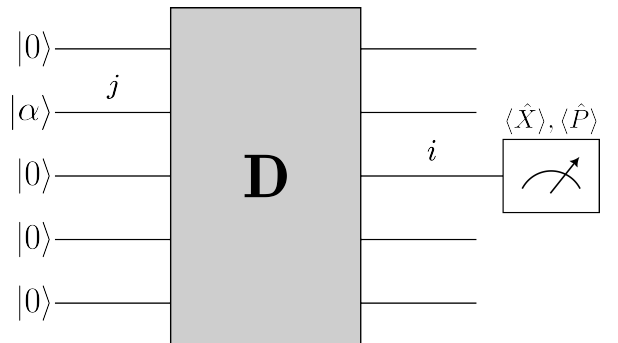


FIG. 1. A schematic for characterizing Gaussian devices. A coherent probe $|\alpha\rangle$ is input into the j^{th} mode of a device D . After the probe evolves through the device, output quadratures are measured in each output mode.

As shown in Fig. 1, the setup consists of a Gaussian device D with N input and output modes. A

well-characterized coherent probe is sent into the j^{th} input mode of the device and vacuum states are input into every other mode. The coherent probe then transforms through the device following the map of Eq. (5). Quadratures are measured at the i^{th} output mode, either by homodyne detection or by heterodyne detection. This process is repeated for all combinations of $i, j \in \{1, 2, \dots, N\}$.

IV. CHARACTERIZATION OF GAUSSIAN PROCESSES

We now outline our method for characterizing Gaussian processes. This involves finding all $4N^2$ real elements of S .

When a coherent probe is input to the j^{th} input mode and vacuum states input into every other mode, the input mean vector is

$$\mathbf{r}^{\text{in}} = (0, \dots, \langle \hat{X}_j \rangle^{\text{in}}, 0, \dots, \langle \hat{P}_j \rangle^{\text{in}}, \dots, 0)^T. \quad (8)$$

This state then evolves via the linear map of Eq. (5) representing the device. Subsequently, the output mean vector \mathbf{r}^{out} will be

$$\mathbf{r}^{\text{out}} = \langle \hat{X}_j \rangle^{\text{in}} \begin{pmatrix} S_{1,j} \\ S_{2,j} \\ \vdots \\ S_{2N,j} \end{pmatrix} + \langle \hat{P}_j \rangle^{\text{in}} \begin{pmatrix} S_{1,N+j} \\ S_{2,N+j} \\ \vdots \\ S_{2N,N+j} \end{pmatrix}. \quad (9)$$

By controlling the phase of the input coherent state, we may choose either $\langle \hat{X}_j \rangle^{\text{in}}$ or $\langle \hat{P}_j \rangle^{\text{in}}$ to be zero independently of the other. In both of these cases, each measurement of an output quadrature is related to a single element of S .

For instance, in order to find the element $S_{i,j}$ where $i, j \in \{1, 2, \dots, N\}$, we send in a coherent state $|\alpha\rangle$ where $\alpha \in \mathbb{R}$ to the input mode j . Subsequently, we measure the position quadrature in mode i , i.e. $\langle \hat{X}_i \rangle^{\text{out}}$. Following Eq. (9), and noting that $\langle \hat{P}_j \rangle^{\text{in}} = 0$, this measurement yields

$$\begin{aligned} \langle \hat{X}_i \rangle^{\text{out}} &= \langle \hat{X}_j \rangle^{\text{in}} S_{i,j} \\ &= \sqrt{2}\alpha S_{i,j} \end{aligned} \quad (10)$$

This relation enables one to directly obtain the matrix element $S_{i,j}$ as

$$S_{i,j} = \frac{\langle \hat{X}_i \rangle^{\text{out}}}{\sqrt{2}\alpha} \quad (11)$$

Likewise, we obtain $S_{N+i,j}$ where $i, j \in \{1, 2, \dots, N\}$ by measuring the momentum quadrature instead, i.e. $\langle \hat{P}_i \rangle^{\text{out}}$.

A similar process yields the elements $S_{i,N+j}$ and $S_{N+i,N+j}$ as well. To do this, we probe the device with an

input coherent state $|i\alpha\rangle$ where $\alpha \in \mathbb{R}$, i.e. $\langle \hat{X}_j \rangle^{\text{in}} = 0$. Measuring the position and momentum quadratures at the output then yields these elements.

Finally, we determine all elements of S by choosing all combinations of input modes j and output modes i . Fig. 2 shows the measurement settings necessary to find all elements of S , requiring $4N^2$ measurement settings in total.

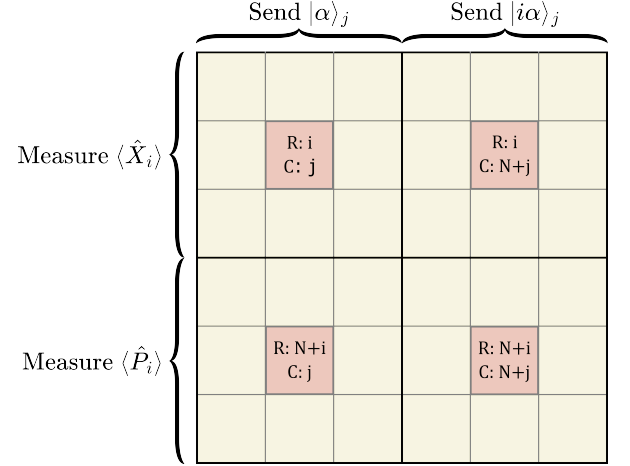


FIG. 2. Figure shows the probes and measurement settings needed to find the elements of the matrix S . R denotes row number and C denotes column number. Four elements of the matrix can be determined for a given input and output mode by changing the phase of the probe as well as the quadrature measured.

A. Simplification for passive transformations

Passive transformations, such as those in linear optics, can be characterized by $O(N^2)$ parameters in the form of a $N \times N$ unitary matrix U . Noticing the relation of U to S in Eq. (7), we can reduce the number of measurements required to completely characterize U . For instance, by restricting the input coherent states to be of the form $|\alpha\rangle$ where $\alpha \in \mathbb{R}$, one can find all the elements of $\text{Re}(U)$ and $\text{Im}(U)$. The unitary matrix can then be reconstructed as $\text{Re}(U) + i\text{Im}(U)$. Thus, only $2N^2$ measurement settings are needed to characterize an N -mode linear optical device.

V. MODELING LOSS

In this section, we account for loss that is inevitable in any experiment. We consider a uniform (or balanced) loss model, where loss is the same in each mode. Such loss is modeled by a set of fictitious beam splitters of the same transmissivity $\eta \in (0, 1]$ attached to each input mode of the device [25]. Vacuum is input into all of the ancillary modes. A schematic of this loss model is shown in Fig. 3.

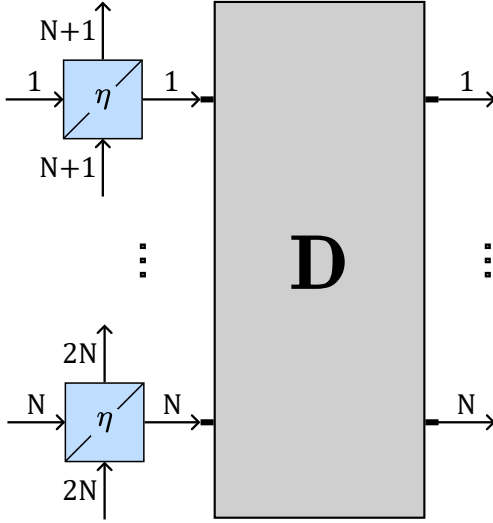


FIG. 3. Balanced loss model with fictitious beam splitters of the same transmissivity η at the input. For each input mode j , we label the ancillary mode of the fictitious beam splitter as $N + j$. The ancillary modes $\{N + 1, \dots, 2N\}$ have vacuum as input.

It was shown in Ref. [26] that uniform loss commutes with passive linear optical transformations. As shown in Appendix B, uniform loss commutes with the Gaussian map of Eq. (5) also. Therefore, this loss model is agnostic to the position of loss in any device with uniform loss. This allows us to transfer any uniform loss within the device to its input. Thus, the effect of uniform loss is to attenuate the input coherent probe $|\alpha\rangle_j$ to $|\sqrt{\eta}\alpha\rangle_j$. Consequently, Eq. (9) is modified to include the loss as

$$\mathbf{r}^{\text{out}} = \sqrt{\eta}\langle\hat{X}_j\rangle^{\text{in}} \begin{pmatrix} S_{1,j} \\ S_{2,j} \\ \vdots \\ S_{2N,j} \end{pmatrix} + \sqrt{\eta}\langle\hat{P}_j\rangle^{\text{in}} \begin{pmatrix} S_{1,N+j} \\ S_{2,N+j} \\ \vdots \\ S_{2N,N+j} \end{pmatrix} \quad (12)$$

Therefore, following the procedure of section IV yields an experimentally obtained matrix \tilde{S} . \tilde{S} is related to the true symplectic matrix S by $\tilde{S} = \sqrt{\eta}S$. By considering that $\det(S) = 1$, we obtain the transmissivity η as

$$\det(\tilde{S}) = (\sqrt{\eta})^{2N} \det(S) = \eta^N. \quad (13)$$

Thus, η is directly determined from experimental data, thereby requiring no additional measurements. Once determined, η is used to obtain S from the experimentally obtained matrix \tilde{S} as $S = \frac{1}{\sqrt{\eta}}\tilde{S}$. This procedure is summarized in Algorithm 1.

A similar method to characterize loss can be employed for passive linear optical transformations, as the determinant of a unitary transformation also has unit modulus.

Algorithm 1 Algorithm for reconstructing S

```

1: procedure RECONSTRUCTGAUSSIANPROCESS
2:   for  $j \in \{1, \dots, N\}$  and  $\alpha \in \mathbb{R}$  do
3:     Probe  $j^{\text{th}}$  mode with  $|\alpha\rangle$ 
4:     Evolve  $|\alpha\rangle$  through the unknown device
5:     Measure  $\langle\hat{X}\rangle$  and  $\langle\hat{P}\rangle$  over all output modes
6:     Reconstruct  $j^{\text{th}}$  column of  $\tilde{S}$ 
7:     Probe the  $j^{\text{th}}$  mode with  $|i\alpha\rangle$ 
8:     Evolve  $|i\alpha\rangle$  through the unknown device
9:     Measure  $\langle\hat{X}\rangle$  and  $\langle\hat{P}\rangle$  over all output modes
10:    Reconstruct the  $(j + N)^{\text{th}}$  column of  $\tilde{S}$ 
11:  end for
12:  Calculate  $\eta = \det(\tilde{S})^{\frac{1}{N}}$ 
13:  Calculate  $S = \frac{1}{\sqrt{\eta}}\tilde{S}$ 
14: end procedure

```

VI. SIMULATION

To test the validity of our method, we simulate it on Strawberry Fields, an open-source Python library for quantum continuous variable systems [27, 28]. The corresponding Python code used for the simulation is available on GitHub at [29].

We randomly generated symplectic matrices S^{rand} for N -mode devices where N varied from 2 to 20. For each case, we implemented the corresponding Gaussian transformation and uniform loss. We then reconstructed those devices using either homodyne or heterodyne detection to obtain S^{recon} . The accuracy of reconstruction was quantified by a scaled Frobenius (Hilbert–Schmidt) norm of the difference between the randomly generated matrix and the reconstructed matrix. This norm is defined as

$$F = \frac{1}{N} \|S^{\text{rand}} - S^{\text{recon}}\|_F = \frac{1}{N} \sqrt{\sum_{i,j} |S_{i,j}^{\text{rand}} - S_{i,j}^{\text{recon}}|^2}, \quad (14)$$

where N is the number of modes. A lower value of F indicates a more accurate reconstruction. We repeated this process 500 times and calculated the average of this norm for each choice of N .

In our simulation, we used coherent probes of amplitude $\alpha = 1000$. The transmissivity η was set at either 0% or at 50%. We ensured that the same number of coherent probes were used in both homodyne and heterodyne reconstruction. This was necessary because homodyne reconstruction requires two probes to measure both quadratures while heterodyne only requires one.

The results of the simulation are shown in Fig. 4. We note that the value of the scaled Frobenius norm is independent of the number of modes of the device. This indicates that our method is readily scalable with the size of the reconstructed device. We also notice that heterodyne reconstruction outperforms homodyne reconstruction. This is supported by two observations. First, for

each value of the loss parameter, heterodyne reconstruction yields a lower value of the scaled Frobenius norm than that of homodyne reconstruction. Second, the uncertainties in the homodyne data are larger than those in heterodyne data.

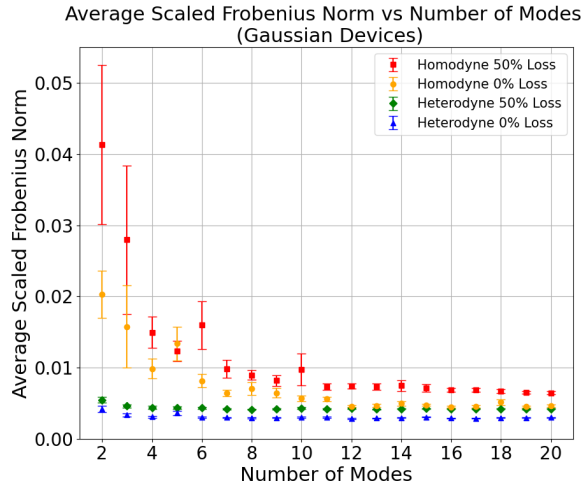


FIG. 4. Average scaled Frobenius norm of the difference between the randomly generated symplectic matrix and its reconstruction. Reconstruction was performed using both heterodyne and homodyne measurements. The loss parameter was set either at 0% or at 50%. Heterodyne reconstruction is observed to outperform homodyne reconstruction.

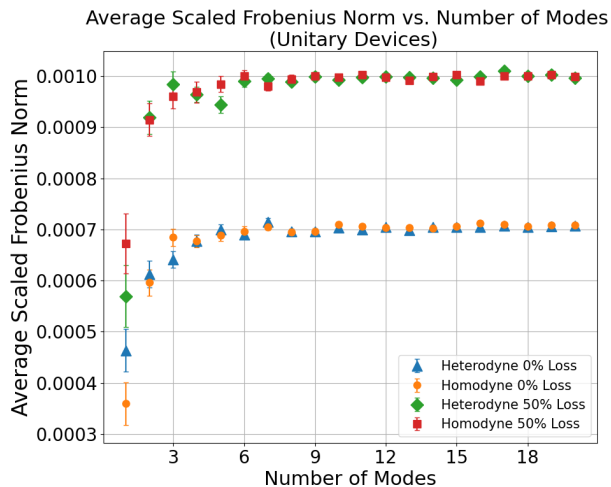


FIG. 5. Average scaled Frobenius norm of the difference between the randomly generated unitary matrix and its reconstruction. Reconstruction was performed using both heterodyne and homodyne measurements for lossless and lossy linear devices. The norm is observed to be similar for both homodyne and heterodyne reconstruction.

A similar simulation was performed for linear processes. In this simulation, unitary matrices were randomly sampled from the Haar measure. After recon-

struction, the scaled Frobenius norm of the difference between the random unitary and the reconstructed unitary was computed. This task was repeated 50 times and the average scaled Frobenius norm was calculated.

The results of this simulation are shown in Fig. 5. As in the case of Gaussian devices, the accuracy of reconstruction is observed to be independent of the number of modes of the device, thereby indicating the scalability of the procedure. However, we observe that both homodyne detection and heterodyne detection reconstruct linear devices equally well.

VII. DISCUSSION

The results of the simulation in Sec. VI demonstrate the superiority of heterodyne measurements for reconstructing Gaussian processes but not for linear processes. We now consider why this might be the case.

We suggest that the superiority of heterodyne reconstruction is explained by the nature of the quantum state on which quadrature measurements are performed. In the context of quantum state reconstruction, it was shown in Ref. [24] that both heterodyne detection and homodyne detection perform equally well in reconstructing the first moments of any minimum-uncertainty state. However, if the state is not a minimum-uncertainty state, heterodyne reconstruction performs better. This result is directly relevant to our method, as our reconstruction is dependent on measuring the first moment of the output state of the unknown process.

While characterizing linear processes, the output state of our method is a minimum-uncertainty state, as linear processes map coherent probes to other coherent states. In contrast, the output state for a Gaussian process is not a minimum-uncertainty state, as Gaussian devices map coherent probes to other Gaussian states in general. This difference in the nature of the output states explains the superiority of heterodyne measurements in reconstructing Gaussian processes.

VIII. CONCLUSION

We have presented a method for characterizing Gaussian quantum processes using only Gaussian resources. Our approach directly reconstructs the symplectic matrix that describes an arbitrary Gaussian process, requiring only $O(N^2)$ measurements for an N -mode system. As this method uses only experimentally accessible resources such as coherent probes and quadrature detection methods, it is well-suited for implementation in current experimental setups. A highlight of this method is that it is resilient to uniform loss.

Our results indicate that heterodyne detection outperforms homodyne detection in reconstructing Gaussian processes. However, for linear optical transformations,

both detection methods yield similar results. This observation suggests that heterodyne measurements may prove to be advantageous in a wider variety of tasks in quantum information processing.

IX. ACKNOWLEDGEMENTS

KVJ acknowledges support from Wheaton College via the G. W. Aldeen Grant as well as the Junior Faculty Alumni Grant.

-
- [1] U. Andersen, G. Leuchs, and C. Silberhorn, *Laser & Photonics Reviews* **4**, 337 (2010).
- [2] S. L. Braunstein and P. van Loock, *Rev. Mod. Phys.* **77**, 513 (2005).
- [3] F. Raffaelli, G. Ferranti, D. H. Mahler, P. Sibson, J. E. Kennard, A. Santamato, G. Sinclair, D. Bonneau, M. G. Thompson, and J. C. F. Matthews, *Quantum Science and Technology* **3**, 025003 (2018).
- [4] L. S. Madsen, F. Laudenbach, M. F. Askarani, F. Rortais, T. Vincent, J. F. F. Bulmer, F. M. Miatto, L. Neuhaus, L. G. Helt, M. J. Collins, A. E. Lita, T. Gerrits, S. W. Nam, V. D. Vaidya, M. Menotti, I. Dhand, Z. Vernon, N. Quesada, and J. Lavoie, *Nature* **606**, 75 (2022).
- [5] S.-H. Tan and P. P. Rohde, *Reviews in Physics* **4**, 100030 (2019).
- [6] C. Weedbrook, S. Pirandola, R. García-Patrón, N. J. Cerf, T. C. Ralph, J. H. Shapiro, and S. Lloyd, *Rev. Mod. Phys.* **84**, 621 (2012).
- [7] C. M. Caves, *Phys. Rev. D* **26**, 1817 (1982).
- [8] S. L. Braunstein, *Phys. Rev. A* **71**, 055801 (2005).
- [9] A. Peruzzo, A. Laing, A. Politi, T. Rudolph, and J. L. O’Brien, *Nature Communications* **2**, 224 (2011).
- [10] A. Laing and J. L. O’Brien, (2012), [arXiv:1208.2868 \[quant-ph\]](https://arxiv.org/abs/1208.2868).
- [11] I. Dhand, A. Khalid, H. Lu, and B. C. Sanders, *Journal of Optics* **18**, 035204 (2016).
- [12] X.-Q. Zhou, H. Cable, R. Whittaker, P. Shadbolt, J. L. O’Brien, and J. C. F. Matthews, *Optica* **2**, 510 (2015).
- [13] S. Rahimi-Keshari, M. A. Broome, R. Fickler, A. Fedrizzi, T. C. Ralph, and A. G. White, *Opt. Express* **21**, 13450 (2013).
- [14] D. Suess, N. Maraviglia, R. Kueng, A. Maïnos, C. Sparrow, T. Hashimoto, N. Matsuda, D. Gross, and A. Laing, (2020), [arXiv:2010.00517 \[physics.optics\]](https://arxiv.org/abs/2010.00517).
- [15] F. Hoch, T. Giordani, N. Spagnolo, A. Crespi, R. Osellame, and F. Sciarrino, *Advanced Photonics Nexus* **2**, 016007 (2023).
- [16] K. V. Jacob, A. E. Mirasola, S. Adhikari, and J. P. Dowling, *Phys. Rev. A* **98**, 052327 (2018).
- [17] X.-B. Wang, Z.-W. Yu, J.-Z. Hu, A. Miranowicz, and F. Nori, *Physical Review A* **88** (2013), 10.1103/physreva.88.022101.
- [18] C. Kumar, R. Sengupta, and Arvind, *Phys. Rev. A* **102**, 012616 (2020).
- [19] Y. S. Teo, K. Park, S. Shin, H. Jeong, and P. Marek, *New Journal of Physics* **23**, 063024 (2021).
- [20] X.-B. Wang, T. Hiroshima, A. Tomita, and M. Hayashi, *Physics Reports* **448**, 1 (2007).
- [21] G. Adesso, S. Ragy, and A. R. Lee, *Open Systems & Information Dynamics* **21**, 1440001 (2014).
- [22] A. Serafini, *Quantum Continuous Variables: A Primer of Theoretical Methods* (CRC Press, 2017) pp. 84–87.
- [23] K. Valson Jacob, *On Characterizing Quantum Processes and Detectors*, Ph.D. thesis, Louisiana State University and Agricultural and Mechanical College (2020).
- [24] Y. S. Teo, C. R. Müller, H. Jeong, Z. Hradil, J. Řeháček, and L. L. Sánchez-Soto, *Phys. Rev. A* **95**, 042322 (2017).
- [25] C. C. Gerry and P. L. Knight, *Introductory Quantum Optics*, 2nd ed. (Cambridge University Press, 2023) pp. 270–272.
- [26] M. Oszmaniec and D. J. Brod, *New Journal of Physics* **20**, 092002 (2018).
- [27] N. Killoran, J. Izaac, N. Quesada, V. Bergholm, M. Amy, and C. Weedbrook, *Quantum* **3**, 129 (2019).
- [28] T. R. Bromley, J. M. Arrazola, S. Jahangiri, J. Izaac, N. Quesada, A. D. Gran, M. Schuld, J. Swinerton, Z. Zabaneh, and N. Killoran, *Quantum Science and Technology* **5**, 034010 (2020).
- [29] L. Grove and K. Valson Jacob, “GaussianOptics,” <https://github.com/LoganGrove/GaussianOptics> (2025), GitHub Repository.

APPENDIX

Appendix A: Unitary and symplectic descriptions of linear optics

Consider a N –mode linear optical device with \hat{a}_i^\dagger (\hat{b}_i^\dagger) as the input (output) modes, where $i \in \{1, 2, \dots, N\}$. Let $\hat{\mathbf{a}}^\dagger$, ($\hat{\mathbf{b}}^\dagger$) be the vector of the input (output) mode operators. The input and output quadrature operators are defined from the mode creation and annihilation operators as

$$\begin{aligned}\hat{\mathbf{X}}^{\text{in}} &= \frac{1}{\sqrt{2}} (\hat{\mathbf{a}} + \hat{\mathbf{a}}^\dagger) \\ \hat{\mathbf{P}}^{\text{in}} &= \frac{1}{\sqrt{2}i} (\hat{\mathbf{a}} - \hat{\mathbf{a}}^\dagger) \\ \hat{\mathbf{X}}^{\text{out}} &= \frac{1}{\sqrt{2}} (\hat{\mathbf{b}} + \hat{\mathbf{b}}^\dagger) \\ \hat{\mathbf{P}}^{\text{out}} &= \frac{1}{\sqrt{2}i} (\hat{\mathbf{b}} - \hat{\mathbf{b}}^\dagger)\end{aligned}\quad (\text{A1})$$

The device implements the unitary transformation

$$\hat{\mathbf{b}}^\dagger = U \hat{\mathbf{a}}^\dagger, \quad (\text{A2})$$

where U is an $N \times N$ unitary matrix. This relation can be alternatively expressed as

$$\hat{\mathbf{b}} = U^* \hat{\mathbf{a}}, \quad (\text{A3})$$

where the elements of U^* are the complex conjugates of the corresponding elements of U . Our aim is to describe

the relation between this unitary matrix and the $2N \times 2N$ symplectic matrix S that also represents the transformation of the quadrature operators as

$$\hat{\mathbf{r}}^{\text{out}} = S \hat{\mathbf{r}}^{\text{in}}. \quad (\text{A4})$$

To this end, let us first define the real and imaginary parts of the unitary matrix U as

$$U = \mathbb{R}\text{e}(U) + i\mathbb{I}\text{m}(U), \quad (\text{A5})$$

where all the elements of the matrices $\mathbb{R}\text{e}(U)$ and $\mathbb{I}\text{m}(U)$ are real.

We now find the output quadrature operators in terms of the input quadrature operators. To this end, we substitute the mode evolution in (A2) into the definition of output quadrature operators in (A1). We obtain

$$\begin{aligned} \hat{\mathbf{X}}^{\text{out}} &= \frac{1}{\sqrt{2}}(\hat{\mathbf{b}} + \hat{\mathbf{b}}^\dagger) \\ &= \frac{1}{\sqrt{2}}(U\hat{\mathbf{a}}^\dagger + U^*\hat{\mathbf{a}}) \\ &= \mathbb{R}\text{e}(U)\frac{(\hat{\mathbf{a}} + \hat{\mathbf{a}}^\dagger)}{\sqrt{2}} + \mathbb{I}\text{m}(U)\frac{(\hat{\mathbf{a}} - \hat{\mathbf{a}}^\dagger)}{\sqrt{2}i} \\ &= \mathbb{R}\text{e}(U)\hat{\mathbf{X}}^{\text{in}} + \mathbb{I}\text{m}(U)\hat{\mathbf{P}}^{\text{in}}. \end{aligned} \quad (\text{A6})$$

Similarly, we obtain

$$\begin{aligned} \hat{\mathbf{P}}^{\text{out}} &= \frac{1}{\sqrt{2}i}(\hat{\mathbf{b}} - \hat{\mathbf{b}}^\dagger) \\ &= \frac{1}{\sqrt{2}i}(U\hat{\mathbf{a}}^\dagger - U^*\hat{\mathbf{a}}) \\ &= -\mathbb{I}\text{m}(U)\frac{(\hat{\mathbf{a}} + \hat{\mathbf{a}}^\dagger)}{\sqrt{2}} + \mathbb{R}\text{e}(U)\frac{(\hat{\mathbf{a}} - \hat{\mathbf{a}}^\dagger)}{\sqrt{2}i} \\ &= -\mathbb{I}\text{m}(U)\hat{\mathbf{X}}^{\text{in}} + \mathbb{R}\text{e}(U)\hat{\mathbf{P}}^{\text{in}}. \end{aligned} \quad (\text{A7})$$

Finally, we combine (A6) and (A7) in matrix form so as to explicitly find the form of the symplectic matrix S .

$$\begin{pmatrix} \hat{\mathbf{X}}^{\text{out}} \\ \hat{\mathbf{P}}^{\text{out}} \end{pmatrix} = \begin{pmatrix} \mathbb{R}\text{e}(U) & \mathbb{I}\text{m}(U) \\ -\mathbb{I}\text{m}(U) & \mathbb{R}\text{e}(U) \end{pmatrix} \begin{pmatrix} \hat{\mathbf{X}}^{\text{in}} \\ \hat{\mathbf{P}}^{\text{in}} \end{pmatrix}. \quad (\text{A8})$$

Comparing (A8) with (A4), we find

$$S = \begin{pmatrix} \mathbb{R}\text{e}(U) & \mathbb{I}\text{m}(U) \\ -\mathbb{I}\text{m}(U) & \mathbb{R}\text{e}(U) \end{pmatrix}. \quad (\text{A9})$$

Appendix B: Uniform loss model in Gaussian devices

Consider a Gaussian quantum device with uniform loss in all modes. This loss is modeled by a set of fictitious beam splitters with the same transmissivity η in each mode. We demonstrate that this type of loss commutes with the device, meaning that all losses can be effectively moved to the beginning of the device. This was shown to be true in Ref. [26] for the restricted case of passive linear optics.

To this end, we consider a device with uniform loss within the device, and another device with uniform losses at the input. A schematic of these devices is shown in Fig. 6. We shall show that the transformations of the mode operators are identical in both these cases.

If the device were to be lossless, then all beam splitters would have transmissivity $\eta = 1$, and the input quadrature operators transform as

$$\hat{\mathbf{r}} \rightarrow S_2 S_1 \hat{\mathbf{r}}. \quad (\text{B1})$$

Consider the scenario where uniform loss occurs within the device. In this case, the input quadrature operators of the device evolve as

$$\hat{\mathbf{r}} \rightarrow S_1 \hat{\mathbf{r}} \rightarrow \sqrt{\eta} S_1 \hat{\mathbf{r}} \rightarrow \sqrt{\eta} S_2 S_1 \hat{\mathbf{r}}. \quad (\text{B2})$$

In the alternate scenario where uniform loss occurs at the beginning of the device, the input quadrature operators evolve as

$$\hat{\mathbf{r}} \rightarrow \sqrt{\eta} \hat{\mathbf{r}} \rightarrow \sqrt{\eta} S_1 \hat{\mathbf{r}} \rightarrow \sqrt{\eta} S_2 S_1 \hat{\mathbf{r}}. \quad (\text{B3})$$

The agreement of (B2) with (B3) shows that uniform loss within a Gaussian device can always be commuted to the beginning of the device.

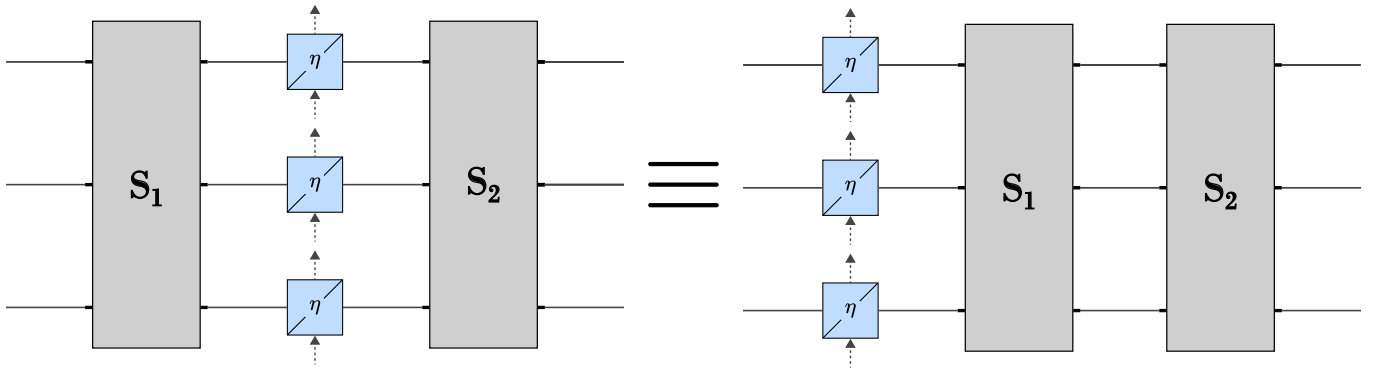


FIG. 6. Schematic of Gaussian devices with uniform loss within and before the device. The transformation of the quadrature operators are identical in both cases.